

Single and Multi-Photon Events with Missing Energy in e^+e^- Collisions at $\sqrt{s} = 189$ GeV

The L3 Collaboration

Abstract

Single and multi-photon events with missing energy are analysed using data collected with the L3 detector at LEP at a centre-of-mass energy of 189 GeV, for a total of 176 pb^{-1} of integrated luminosity. The cross section of the process $e^+e^- \rightarrow \nu\bar{\nu}\gamma(\gamma)$ is measured and the number of light neutrino flavours is determined to be $N_\nu = 3.011 \pm 0.077$ including lower energy data. Upper limits on cross sections of supersymmetric processes are set and interpretations in supersymmetric models provide improved limits on the masses of the lightest neutralino and the gravitino. Graviton-photon production in low scale gravity models with extra dimensions is searched for and limits on the energy scale of the model are set exceeding 1 TeV for two extra dimensions.

Submitted to *Phys. Lett. B*

1 Introduction

In the Standard Model [1] single or multi-photon events with missing energy are produced via the reaction $e^+e^- \rightarrow \nu\bar{\nu}\gamma(\gamma)$ which proceeds through s -channel Z exchange and t -channel W exchange. Searches for single and multi-photon final states as well as measurements of the $e^+e^- \rightarrow \nu\bar{\nu}\gamma(\gamma)$ cross section have already been performed by L3 [2–4] and by other LEP experiments [5] at lower centre-of-mass energies. For the first time, the determination of the number of light neutrino species from single photon events at energies above the Z resonance is reported here.

In supersymmetric models [6] different supersymmetry (SUSY) breaking mechanisms lead to different phenomenologies. The SUSY breaking scale, \sqrt{F} , or equivalently the gravitino mass ($m_{\tilde{G}} = F/[\sqrt{3}/(8\pi)m_P]$ where m_P is the Planck mass), is considered as a free parameter. Three different scenarios are distinguished: heavy, light and superlight gravitinos.

In gravity-mediated SUSY breaking models (SUGRA) the gravitino is heavy ($100 \text{ GeV} \lesssim m_{\tilde{G}} \lesssim 1 \text{ TeV}$) and thus does not play a role in production or decay processes. The lightest neutralino is the lightest supersymmetric particle (LSP), which is stable under the assumption of R -parity [7] conservation and escapes detection due to its weakly interacting nature. In this scenario, single or multi-photon signatures arise from pair-production of neutralinos ($\tilde{\chi}_1^0\tilde{\chi}_2^0$ and $\tilde{\chi}_2^0\tilde{\chi}_2^0$) [8]. Subsequent one-loop decays of $\tilde{\chi}_2^0$ into $\tilde{\chi}_1^0\gamma$ have a branching fraction close to 100% if one of the two neutralinos is pure photino and the other pure higgsino [9]. In general, neutralinos are mixtures of photinos, zinos and higgsinos.

In models with Gauge-Mediated SUSY Breaking (GMSB) [10], a light gravitino ($10^{-2} \text{ eV} \lesssim m_{\tilde{G}} \lesssim 10^2 \text{ eV}$) is the LSP. In this case the gravitino plays a fundamental role in the decay of SUSY particles. In particular, the $\tilde{\chi}_1^0$ is no longer stable and decays through $\tilde{\chi}_1^0 \rightarrow \tilde{G}\gamma$ if it is the next-to lightest supersymmetric particle (NLSP) [11]. Pair-production of the lightest neutralino leads to a two-photon plus missing energy signature in the detector.

When the scale of local supersymmetry breaking is decoupled from the breaking of global supersymmetry as in no-scale supergravity models [12], the gravitino can be superlight ($10^{-6} \text{ eV} \lesssim m_{\tilde{G}} \lesssim 10^{-4} \text{ eV}$). Then, it is produced not only in SUSY particle decays but also directly in pairs [13] or associated with a neutralino [14]. Pair-production of gravitinos accompanied by initial state radiation leads to a single photon signature. This signature also arises in $\tilde{\chi}_1^0\tilde{G}$ production when the neutralino decays radiatively to gravitino and photon.

Recently, it has been proposed that the fundamental gravitational scale in quantum gravity models with extra dimensions is as low as the electroweak scale [15] thus naturally solving the hierarchy problem. Within the framework of these models real gravitons are produced in e^+e^- collisions through the process $e^+e^- \rightarrow \gamma G$, where the graviton escapes undetected leading to a single photon plus missing energy signature.

2 Data Sample and Simulation

In this analysis we use the data collected by the L3 detector [16] during the high energy run of LEP in 1998 corresponding to an integrated luminosity of 176.4 pb^{-1} at an average centre-of-mass energy of $\sqrt{s} = 188.6 \text{ GeV}$, hereafter denoted 189 GeV.

Monte Carlo events for the following Standard Model processes are simulated: $e^+e^- \rightarrow \nu\bar{\nu}\gamma(\gamma)$ with KORALZ [17], $e^+e^- \rightarrow \gamma\gamma(\gamma)$ with GGG [18], Bhabha scattering for large scattering angles with BHWIDE [19], and for small scattering angles with TEEGG [20], and four-fermion final

states specifically the processes $e^+e^- \rightarrow e^+e^-e^+e^-$ with `DIAG36` [21], and $e^+e^- \rightarrow e^+e^-\nu\bar{\nu}$ with `EXCALIBUR` [22].

SUSY processes are simulated with the Monte Carlo program `SUSYGEN` [23] for SUSY particle masses (m_{SUSY}) between zero and the kinematic limit and, in $\tilde{\chi}_1^0$ LSP scenarios, for $\Delta m = m_{\text{SUSY}} - m_{\text{LSP}}$ between 1 GeV and m_{SUSY} . To ensure the radiative decay of the neutralino, the scalar electron (\tilde{e}_R) mass is set to 100 GeV, except for $\tilde{\chi}_1^0\tilde{G}$ production where it is set to 200 GeV. The detector response is simulated using the `GEANT` program [24], which takes into account the effects of energy loss, multiple scattering and showering in the detector.

3 Event Selection

Electrons and photons are measured accurately by the BGO electromagnetic calorimeter. They are required to have an energy greater than 0.9 GeV. The shape of their energy deposition must be consistent with an electromagnetic shower. Electrons are defined as electromagnetic clusters matched with a charged track reconstructed in the central tracking chamber. Identified conversion electrons from photons interacting with the beam pipe or with the silicon microvertex detector, 4% of the total, are also accepted as photons. Bhabha events and $e^+e^- \rightarrow \gamma\gamma(\gamma)$ events that are fully contained in the calorimeter are used to check the particle identification as well as the energy resolution, which is 1% for high energy electrons and photons in both the barrel and the endcaps. The barrel region is defined as the polar angle range $43^\circ < \theta < 137^\circ$ with respect to the beam axis and the endcap region as the polar angle range $14^\circ < \theta < 36^\circ$ or $144^\circ < \theta < 166^\circ$.

3.1 High Energy Photons

The selection of high energy single and multi-photon events requires at least one photon with energy greater than 5 GeV in the barrel or endcaps region. There must be no charged tracks apart from those consistent with photon conversion. The following cuts are imposed to suppress events which do not consist of photons only in the final state. The energy not assigned to identified photons has to be smaller than 10 GeV and the energy measured in the electromagnetic calorimeter between BGO barrel and endcaps must be smaller than 7 GeV. There must be no track in the muon chambers and at most one BGO cluster not identified as a photon.

To reduce the background from radiative Bhabha events with particles escaping along the beam pipe, as well as from the process $e^+e^- \rightarrow \gamma\gamma(\gamma)$, events with less than 20 GeV transverse momentum are rejected if energy is observed in the small polar angle detectors covering an angular range of $1.5^\circ - 11^\circ$. The total transverse momentum of photons is required to be greater than 5 GeV if no second photon with energy greater than 5 GeV is found. If two calorimetric clusters are present and if only one is identified as a photon, their acollinearity must be greater than 5.2° and their acoplanarity must be greater than 2.4° . Furthermore, energy clusters in the hadron calorimeter (HCAL) must have less than 3 GeV energy if a photon is detected with an acoplanarity less than 15° to the HCAL cluster.

When a second photon with energy above 5 GeV is present, the total transverse momentum must be greater than 3 GeV and the recoil mass must be larger than 20 GeV. If the total transverse momentum is smaller than 30 GeV, the acollinearity is required to be larger than 8.1° and the acoplanarity to be larger than 5.2° . If the transverse momentum is smaller than 20 GeV, the missing momentum direction is required to be at least 7° away from the beam pipe. If the acoplanarity is smaller than 2.4° , the recoil mass must be greater than 50 GeV.

To suppress cosmic ray background, we require for photon energies smaller than 15 GeV, that the most energetic photon is not aligned with hits in the muon detector. For photon energies larger than 15 GeV, there must be at least one scintillator time measurement within ± 5 ns of the beam crossing time. Furthermore, an event is rejected if more than 20 hits are found in the central tracking chamber in a 1 cm road between any pair of energy depositions in the BGO.

The number of events with one or more photons is listed in table 1 together with the predicted rates for $\nu\bar{\nu}\gamma(\gamma)$ and other processes originating from e^+e^- collisions. The cosmic ray background in the event sample is estimated from studies of out-of-time events and also listed in table 1. Figure 1 shows the energy spectrum of the most energetic photon normalised to the beam energy for single and multi-photon events.

For the sub-sample of events with two or more photons a minimum energy for the second photon of 1 GeV is required. In the data 21 events are observed compared to a Monte Carlo prediction of 36.2 events, see table 1. For recoil masses larger than 110 GeV we observe 2 events compared to an expectation of 12.7 events. Figure 2(a) shows the two-photon recoil mass distribution. The lack of data compared to the Monte Carlo prediction has been subject to extensive investigations concerning the performance of sub-detectors and triggers used in this analysis. The noise level of sub-detectors is studied using randomly triggered beam-gate events. The performance of the electromagnetic calorimeter is cross-checked with Bhabha events and events from $e^+e^- \rightarrow \gamma\gamma(\gamma)$. Triggers important for single and multi-photon events are investigated using single electron¹⁾ and Bhabha events. The theoretical predictions for the cross section of $e^+e^- \rightarrow \nu\bar{\nu}\gamma\gamma(\gamma)$ obtained from KORALZ and NUNUGPV are found to agree within 5%. No systematic effect is found to explain the low two-photon rate. An independent analysis leads to the same conclusion. Therefore the deficit is treated as a statistical fluctuation.

3.2 Low Energy Photons

This selection extends the energy range for photons down to 1.3 GeV. It covers only the barrel region where a single photon trigger is implemented with a threshold around 900 MeV [25]. There must be no other BGO clusters in barrel or endcaps with more than 200 MeV. The energy in the HCAL must be less than 6 GeV. To reduce the rate of small angle Bhabha scattering no energy deposit is allowed in the forward detectors. Events with a track in the central tracking chamber or in the muon chambers are rejected to reduce the rate of single electron and cosmic muon events. To further reduce cosmic ray events not pointing to the interaction region, cuts on the transverse shape of the photon shower are made. For the simulation of the process $e^+e^- \rightarrow e^+e^-\gamma(\gamma)$ the TEEGG program is used which includes fourth order contributions. In order to use this program, a cut on the transverse momentum of the photon greater than 1.3 GeV is applied [20]. From a study of single electron events its precision is estimated to be at the 20% level. The number of selected events, predictions from e^+e^- collision processes and an estimate of cosmic ray contamination are listed in table 1. Figure 2(b) shows the observed photon energy spectrum compared to Monte Carlo prediction.

¹⁾Radiative Bhabha scattering events where one electron and a photon have a very low polar angle, and only a low energetic electron is scattered with a large polar angle.

4 Neutrino Production

To measure the cross section of the $e^+e^- \rightarrow \nu\bar{\nu}\gamma(\gamma)$ process we restrict the analysis to photon energies above 5 GeV (see table 1) to ensure a good signal to background ratio.

The overall efficiency for $e^+e^- \rightarrow \nu\bar{\nu}\gamma(\gamma)$ events satisfying the kinematic requirements $E_\gamma > 5$ GeV and $|\cos\theta_\gamma| < 0.97$ is 60.77%. This efficiency includes a correction of $(2.58 \pm 0.18)\%$ due to cosmic ray veto requirements, which is estimated by studying single electron events. A correction of $(0.67 \pm 0.07)\%$ due to detector noise sources not properly simulated such as that induced by beam halo in the forward detectors is also included and is quantified using randomly triggered beam-gate events. The systematic error on the efficiency is composed of the errors on the two corrections and several other sources including an error of 0.34% due to photon identification, of 0.60% due to an uncertainty on the amount of converted photons, and 0.21% due to limited Monte Carlo statistics. The total systematic error on the efficiency amounts to 0.75%. The error on the luminosity is 0.4 pb^{-1} and on the total background contamination the error is 2.1 events.

The measured cross section at $\sqrt{s} = 188.6$ GeV is

$$\sigma_{\nu\bar{\nu}\gamma(\gamma)} = 5.25 \pm 0.22 \text{ (stat)} \pm 0.07 \text{ (syst)} \text{ pb}$$

to be compared to the prediction of the Standard Model of 5.28 ± 0.05 pb obtained with KORALZ, where the 1% error accounts for the theoretical uncertainty assigned to this process [26]. This measurement is extrapolated to a total cross section for $e^+e^- \rightarrow \nu\bar{\nu}(\gamma)$ production of 58.3 ± 2.7 pb. The prediction of the Standard Model obtained with KORALZ is 58.6 pb. Figure 3 shows both the $\nu\bar{\nu}\gamma(\gamma)$ cross section measurement and the total neutrino-pair extrapolation versus centre-of-mass energy together with the prediction of the Standard Model and measurements at lower centre-of-mass energies.

To determine the number of light neutrino species a maximum likelihood fit to the photon energy spectra is performed at each centre-of-mass energy above the Z resonance. For each energy interval the theoretical prediction is obtained by linearly interpolating KORALZ predictions for $N_\nu = 1, 2, 3, 4, 5$. Due to the different contributions to the energy spectrum from $\nu_e\bar{\nu}_e$ t -channel production via W exchange and $\nu\bar{\nu}$ s -channel production via Z exchange, this method is more powerful than using the total cross section measurement. In addition to the systematic error from the cross section measurement, the theoretical uncertainty on the photon energy spectrum – estimated by comparing KORALZ with NUNUGPV – is taken into account. The result is $N_\nu = 3.05 \pm 0.11 \pm 0.04$.

A compilation of the measurements at the different centre-of-mass energies is shown in table 2. The precision of this result is comparable with our previous measurement [4] from single photon events around the Z resonance. The combined measurement is

$$N_\nu = 3.011 \pm 0.077.$$

This result is more precise than the present world average on the number of light neutrino families determined with the single photon method [27].

5 Limits on Supersymmetry

The limits derived in the following are obtained from 189 GeV data. They correspond to a confidence level of 95%. Cross section limits are calculated using a likelihood approach [28]

where the spectra of a discriminant variable for data, background and signal simulations are compared.

5.1 Single Photon Signature

For interpretations within SUSY frameworks the low energy photons are included. Here, the discriminant variable used to derive cross section limits is the photon energy.

In the heavy gravitino scenario, the single photon signature arises from the reaction $e^+e^- \rightarrow \tilde{\chi}_2^0 \tilde{\chi}_1^0$, which proceeds through s -channel Z exchange and t -channel scalar electron exchange ($\tilde{e}_{L,R}$). Cross section upper limits shown in figure 4 are set under the assumption of 100% branching fraction for $\tilde{\chi}_2^0 \rightarrow \tilde{\chi}_1^0 \gamma$. Typical detection efficiencies for this process are around 75%.

Also the reaction $e^+e^- \rightarrow \tilde{G} \tilde{\chi}_1^0$ proceeds through s -channel Z exchange and t -channel $\tilde{e}_{L,R}$ exchange. Efficiencies for this process with $\tilde{\chi}_1^0 \rightarrow \tilde{G} \gamma$ range between 64% for $m_{\tilde{\chi}_1^0} = 0.5$ GeV and 79% for $m_{\tilde{\chi}_1^0}$ at the kinematic limit. The cross section upper limit as a function of $m_{\tilde{\chi}_1^0}$ is shown in figure 5(a) together with the expected limit obtained in Monte Carlo trials with background only. The no-scale SUGRA model of [14], referred to as LNZ, has only two free parameters – gravitino and neutralino masses. The neutralino is the NLSP, which is almost pure bino. Here, the dominant decay channel is $\tilde{\chi}_1^0 \rightarrow \tilde{G} \gamma$. The small contribution of the decay into Z for $m_{\tilde{\chi}_1^0} \gtrsim 100$ GeV is taken into account. Figure 5(b) shows exclusion contours in the $m_{\tilde{G}} - m_{\tilde{\chi}_1^0}$ plane.

If $m_{\text{NLSP}} > \sqrt{s}$, the process $e^+e^- \rightarrow \tilde{G} \tilde{G}$ [13] is the only reaction to produce SUSY particles. Accompanied by initial state radiation it leads to single or multi-photon signatures. Following our analysis in [3] a lower limit on the gravitino mass is derived

$$m_{\tilde{G}} > 8.9 \cdot 10^{-6} \text{ eV},$$

corresponding to a lower limit on the SUSY breaking scale of $\sqrt{F} > 192.3$ GeV. The average lower limit for the gravitino mass obtained in Monte Carlo trials with background only is $9.7 \cdot 10^{-6}$ eV.

5.2 Multi-Photon Signature

Using a binned likelihood technique, the discriminant variable is constructed for the multi-photon events combining the energies of the two most energetic photons, their polar angles, recoil mass, and the polar angle of the missing momentum vector. For each event class, background and signal Monte Carlo processes, denoted by j , and each input quantity i , a probability density function f_j^i is computed and the discriminant variable of an event is then given by

$$F(\vec{x}) = \frac{\prod_i p_{\text{signal}}^i(x_i)}{\sum_j \prod_i p_j^i(x_i)} \quad \text{with} \quad p_j^i(x_i) = \frac{f_j^i(x_i)}{\sum_k f_k^i(x_i)},$$

where x_i are the measured values of the six input variables of an event. The distribution of the discriminant is shown in figure 6 for $\tilde{\chi}_1^0 \tilde{\chi}_1^0 \rightarrow \tilde{G} \tilde{G} \gamma \gamma$ with $m_{\tilde{\chi}_1^0} = 90$ GeV. The discrepancy between measurement and Standard Model prediction is located in the background and not in the signal region. This holds also for the other mass points and for the heavy gravitino scenario.

In the heavy gravitino scenario, a two-photon signature is produced by the process $e^+e^- \rightarrow \tilde{\chi}_2^0 \tilde{\chi}_2^0$ and subsequent decay to $\tilde{\chi}_1^0 \gamma$. Typical efficiencies for this process are around 64%. Cross section upper limits are obtained as shown in figure 7(a). The interpretation of the $ee\gamma\gamma$ event

with large transverse missing energy observed by CDF [29] suggests a high branching ratio for the radiative decay of the $\tilde{\chi}_2^0$ in the heavy gravitino scenario, which can be achieved if $\tilde{\chi}_2^0$ is a pure photino and $\tilde{\chi}_1^0$ is a pure higgsino. With this assumption, the lower mass limit of $\tilde{\chi}_2^0$ as a function of the scalar electron mass is calculated for mass differences between $\tilde{\chi}_2^0$ and $\tilde{\chi}_1^0$ greater than 10 GeV as shown in figure 7(b). For each $\tilde{\chi}_2^0$ mass, the exclusion is obtained using the most conservative cross section upper limit for any $\Delta m > 10$ GeV. The regions kinematically allowed [30] for the CDF event are overlaid in figure 7(b). The two exclusions obtained for equal masses of $\tilde{e}_{L,R}$ and for $m_{\tilde{e}_L} \gg m_{\tilde{e}_R}$ are shown in the interesting mass range for $m_{\tilde{e}_R}$.

The selection described in this paper is devised for photons originating from the interaction point. For a neutralino mean decay length $d_{\tilde{\chi}_1^0}$ larger than 1 cm the experimental sensitivity drops. This problem arises only for peculiar situations in the light gravitino scenario. The following limits in the gravitino LSP scenario are derived under the assumption of $d_{\tilde{\chi}_1^0} < 1$ cm. The cross section limits for the process $e^+e^- \rightarrow \tilde{\chi}_1^0\tilde{\chi}_1^0 \rightarrow \tilde{G}\tilde{G}\gamma\gamma$ are displayed in figure 8(a) versus neutralino mass. The efficiency varies between 17% for $m_{\tilde{\chi}_1^0} = 0.5$ GeV and 62% for $m_{\tilde{\chi}_1^0} = 94$ GeV. Theoretical predictions for two extreme cases of neutralino content²⁾ [31], which determines its coupling to the photon, are shown in the same figure. For these cases of neutralino composition and for a pure photino, we derive lower limits on the mass of the lightest neutralino as listed in table 3. Figure 8(b) shows the exclusion in the $\tilde{\chi}_1^0 - \tilde{e}_{L,R}$ mass plane derived with our data for a neutralino being pure bino. The $ee\gamma\gamma$ event observed by CDF also has an interpretation in supersymmetric models with gravitino LSP [31]. Our analysis almost rules out this interpretation as shown in figure 8(b).

In minimal models with gauge-mediated SUSY breaking only five parameters determine the sparticle sector of the theory [10]. The parameters are Λ , the scale of SUSY breaking in the messenger sector, M_m , the messenger mass scale, N_m , the number of messenger fields, $\tan\beta$, the ratio of Higgs vacuum expectation values. In this model the absolute value of μ , the higgsino mass term, is fixed, however its sign is a free parameter. They have been scanned to obtain neutralino masses, pair-production cross sections and branching ratios for the decay to gravitino and photon. The scan ranges on the individual parameters are [32] $10 \text{ TeV} \leq \Lambda \leq 100 \text{ TeV}$, $\Lambda/0.9 \leq M_m \leq \Lambda/0.01$, $N_m = 1 \dots 4$, $1 \leq \tan\beta \leq 60$, $\text{sign}\mu = \pm 1$. The program ISASUSY [33] has been used to calculate sparticle masses and couplings from GMSB model parameters, and SUSYGEN to derive from these numbers the cross section for neutralino pair-production including initial state radiation. Assuming a neutralino NLSP scenario, the minimal cross section of $\tilde{\chi}_1^0\tilde{\chi}_1^0$ production obtained within GMSB is shown in figure 8(a), which leads to a lower limit of

$$m_{\tilde{\chi}_1^0} > 88.2 \text{ GeV} .$$

6 Limits on Graviton Production

Massive spin 2 gravitons propagating in $4+\delta$ dimensions interact with Standard Model particles with sizable strength in low scale gravity models with extra dimensions [15]. Gravitons produced via $e^+e^- \rightarrow \gamma G$ lead to a single photon and missing energy signature, since the graviton is not observed in the detector. The reaction proceeds through s -channel photon exchange, t -channel electron exchange and four-particle contact interaction [34].

²⁾For the higgsino case a 2% photino component is required to ensure the decay into $\gamma\tilde{G}$.

To convert the theoretical cross section of this process [34] into an estimate on the number of events expected from graviton production, the differential cross section in energy and angle has been multiplied by efficiency and luminosity. The efficiency is derived from $\nu\bar{\nu}\gamma(\gamma)$ Monte Carlo simulation in a grid in the $E_\gamma - \cos\theta_\gamma$ plane for $E_\gamma > 4$ GeV. The efficiency for $e^+e^- \rightarrow \gamma G$ within $E_\gamma > 4$ GeV and $\cos\theta_\gamma < 0.97$ is listed in table 4 for $2 \leq \delta \leq 10$. The energy spectra shown in figure 1(b) and 2(b) are used to derive upper limits on the cross section. They are listed in table 4 together with the corresponding values for the energy scale M_D . These bounds improve on our previously published limits [35].

7 Acknowledgements

We wish to express our gratitude to the CERN accelerator division for the excellent performance of the LEP machine. We acknowledge the effort of the engineers and technicians who have participated in the construction and maintenance of this experiment.

References

- [1] S.L. Glashow, Nucl. Phys. **22** (1961) 579;
S. Weinberg, Phys. Rev. Lett. **19** (1967) 1264;
A. Salam, *Elementary Particle Theory*, Ed. N. Svartholm, Stockholm, Almquist and Wiksell (1968), 367.
- [2] L3 Collab., M. Acciarri *et al.*, Phys. Lett. **B 415** (1997) 299.
- [3] L3 Collab., M. Acciarri *et al.*, Phys. Lett. **B 444** (1998) 503.
- [4] L3 Collab., M. Adeva *et al.*, Phys. Lett. **B 275** (1992) 209;
L3 Collab., M. Adriani *et al.*, Phys. Lett. **B 292** (1992) 463;
L3 Collab., M. Acciarri *et al.*, Phys. Lett. **B 431** (1998) 199.
- [5] ALEPH Collab., D. Buskulic *et al.*, Phys. Lett. **B 313** (1993) 520;
ALEPH Collab., R. Barate *et al.*, Phys. Lett. **B 429** (1998) 201;
DELPHI Collab., P. Abreu *et al.*, Phys. Lett. **B 380** (1996) 471;
DELPHI Collab., P. Abreu *et al.*, Z. Phys. **C 74** (1997) 577;
OPAL Collab., R. Akers *et al.*, Z. Phys. **C 65** (1995) 47;
OPAL Collab., K. Ackerstaff *et al.*, Eur. Phys. J. **C 2** (1998) 607;
OPAL Collab., K. Ackerstaff *et al.*, Eur. Phys. J. **C 8** (1999) 23.
- [6] Y.A. Golfand and E.P. Likhtman, Sov. Phys. JETP **13** (1971) 323;
D.V. Volkhov and V.P. Akulov, Phys. Lett. **B 46** (1973) 109;
J. Wess and B. Zumino, Nucl. Phys. **B 70** (1974) 39;
P. Fayet and S. Ferrara, Phys. Rep. **C 32** (1977) 249;
A. Salam and J. Strathdee, Fortschr. Phys. **26** (1978) 57.
- [7] P. Fayet, Nucl. Phys. **B 90** (1975) 104;
A. Salam and J. Strathdee, Nucl. Phys. **B 87** (1975) 85.
- [8] A. Bartl, H. Fraas and W. Majerotto, Nucl. Phys. **B 278** (1986) 1;
S. Ambrosanio and B. Mele, Phys. Rev. **D 52** (1995) 3900.
- [9] P. Fayet, Phys. Lett. **B 117** (1982) 460;
H.E. Haber and D. Wyler, Nucl. Phys. **B 323** (1989) 267;
S. Ambrosanio and B. Mele, Phys. Rev. **D 53** (1996) 2541;
S. Ambrosanio *et al.*, Phys. Rev. Lett. **76** (1996) 3498.
- [10] M. Dine and A.E. Nelson, Phys. Rev. **D 48** (1993) 1277;
M. Dine, A.E. Nelson and Y. Shirman, Phys. Rev. **D 51** (1995) 1362;
M. Dine, A.E. Nelson, Y. Nir and Y. Shirman, Phys. Rev. **D 53** (1996) 2658.
- [11] J. Ellis and J.S. Hagelin, Phys. Lett. **B 122** (1983) 303;
J. Ellis *et al.*, Phys. Lett. **B 147** (1984) 99;
P. Fayet, Phys. Lett. **B 175** (1986) 471;
S. Dimopoulos *et al.*, Phys. Rev. Lett. **76** (1996) 3494;
D.R. Stump *et al.*, Phys. Rev. **D 54** (1996) 1936.

- [12] E. Cremmer, S. Ferrara, C. Kounnas and D.V. Nanopoulos, Phys. Lett. **B 133** (1983) 61;
 J. Ellis, A. Lahanas, D.V. Nanopoulos and K. Tamvakis, Phys. Lett. **B 134** (1984) 429;
 J. Ellis, C. Kounnas and D.V. Nanopoulos, Nucl. Phys. **B 241** (1984) 406;
 J. Ellis, C. Kounnas and D.V. Nanopoulos, Nucl. Phys. **B 247** (1984) 373;
 J. Ellis, K. Enqvist and D.V. Nanopoulos, Phys. Lett. **B 147** (1984) 99.
- [13] A. Brignole, F. Feruglio and F. Zwirner, Nucl. Phys. **B 516** (1998) 13.
- [14] J.L. Lopez, D.V. Nanopoulos and A. Zichichi, Phys. Rev. Lett. **77** (1996) 5168;
 J.L. Lopez, D.V. Nanopoulos and A. Zichichi, Phys. Rev. **D 55** (1997) 5813.
- [15] N. Arkani-Hamed, S. Dimopoulos and G. Dvali, Phys. Lett. **B 429** (1998) 263.
- [16] L3 Collab., B. Adeva *et al.*, Nucl. Instr. and Meth. **A 289** (1990) 35;
 M. Chemarin *et al.*, Nucl. Instr. and Meth. **A 349** (1994) 345;
 M. Acciarri *et al.*, Nucl. Instr. and Meth. **A 351** (1994) 300;
 G. Basti *et al.*, Nucl. Instr. and Meth. **A 374** (1996) 293;
 I.C. Brock *et al.*, Nucl. Instr. and Meth. **A 381** (1996) 236;
 A. Adam *et al.*, Nucl. Instr. and Meth. **A 383** (1996) 342.
- [17] The KORALZ version 4.03 is used.
 S. Jadach, B.F.L. Ward and Z. Wąs, Comp. Phys. Comm. **79** (1994) 503.
- [18] F.A. Berends and R. Kleiss, Nucl. Phys. **B 186** (1981) 22.
- [19] S. Jadach *et al.*, Phys. Lett. **B 390** (1997) 298.
- [20] The TEEGG version 7.1 is used.
 D. Karlen, Nucl. Phys. **B 289** (1987) 23.
- [21] F.A. Berends, P.H. Daverfeldt and R. Kleiss, Nucl. Phys. **B 253** (1985) 441.
- [22] F.A. Berends, R. Pittau and R. Kleiss, Comp. Phys. Comm. **85** (1995) 437.
- [23] S. Katsanevas and P. Morawitz, Comp. Phys. Comm. **112** (1998) 227.
- [24] The L3 detector simulation is based on GEANT Version 3.15.
 See R. Brun *et al.*, *GEANT 3*, CERN DD/EE/84-1 (Revised), September 1987.
 The GHEISHA program (H. Fesefeldt, RWTH Aachen Report PITHA 85/02 (1985)) is used
 to simulate hadronic interactions.
- [25] R. Bizzarri *et al.*, Nucl. Inst. Meth. **A 317** (1992) 463.
- [26] G. Montagna, M. Moretti, O. Nicosini and F. Piccinini, Nucl. Phys. **B 541** (1999) 31.
- [27] C. Caso *et al.*, *Review of Particle Physics*, Eur. Phys. J. **C 3** (1998) 1.
- [28] A. Favara and M. Pieri, *Confidence level estimation and analysis optimisation*, Preprint
 DFF-278/4/1997, E-preprint hep-ex 9706016.
- [29] CDF Collab., F. Abe *et al.*, Phys. Rev. Lett. **81** (1998) 1791.
- [30] S. Ambrosanio, G. Kane, G. Kribs, S. Martin and S. Mrenna, Phys. Rev. **D 55** (1996)
 1372.

- [31] J.L. Lopez and D.V. Nanopoulos, Phys. Rev. **D 55** (1997) 4450.
- [32] S. Ambrosanio, G.D. Kribs and S.P. Martin, Phys. Rev. **D 56** (1997) 1761.
- [33] H. Baer, F. Paige, S.D. Protopopescu and X. Tata, in Proceedings of the Workshop on Physics at Current Accelerators and Supercolliders, Argonne, Ill., Jun 2-5, 1993, ed. J.L. Hewitt, A.R. White and D. Zeppenfeld, (Argonne National Laboratory, 1993), p. 703.
- [34] G.F. Giudice, R. Rattazzi and J.D. Wells, Nucl. Phys. **B 544** (1999) 3.
- [35] L3 Collab., M. Acciarri *et al.*, *Search for Low Scale Gravity Effects in e^+e^- Collisions at LEP*, 1999, Preprint CERN-EP/99-117, Accepted by Phys. Lett. **B**.

The L3 Collaboration:

M.Acciarri,²⁶ P.Achard,¹⁹ O.Adriani,¹⁶ M.Aguilar-Benitez,²⁵ J.Alcaraz,²⁵ G.Alemanni,²² J.Allaby,¹⁷ A.Aloisio,²⁸ M.G.Alvigi,²⁸ G.Ambrosi,¹⁹ H.Anderhub,⁴⁷ V.P.Andreev,^{6,36} T.Angelescu,¹² F.Anselmo,⁹ A.Arefiev,²⁷ T.Azmoon,³ T.Aziz,¹⁰ P.Bagnaia,³⁵ L.Baksay,⁴² A.Balandras,⁴ R.C.Ball,³ S.Banerjee,¹⁰ Sw.Banerjee,¹⁰ A.Barczyk,^{47,45} R.Barillère,¹⁷ L.Barone,³⁵ P.Bartalini,²² M.Basile,⁹ R.Battiston,³² A.Bay,²² F.Becattini,¹⁶ U.Becker,¹⁴ F.Behner,⁴⁷ L.Bellucci,¹⁶ J.Berdugo,²⁵ P.Berges,¹⁴ B.Bertucci,³² B.L.Betev,⁴⁷ S.Bhattacharya,¹⁰ M.Biasini,³² A.Biland,⁴⁷ J.J.Blaising,⁴ S.C.Blyth,³³ G.J.Bobbink,² A.Böhm,¹ L.Boldizar,¹³ B.Borgia,³⁵ D.Bourilkov,⁴⁷ M.Bourquin,¹⁹ S.Braccini,¹⁹ J.G.Branson,³⁸ V.Brigljevic,⁴⁷ F.Brochu,⁴ A.Buffini,¹⁶ A.Buijs,⁴³ J.D.Burger,¹⁴ W.J.Burger,³² J.Busenitz,⁴² A.Button,³ X.D.Cai,⁴ M.Campanelli,⁴⁷ M.Capell,¹⁴ G.Cara Romeo,⁹ G.Carlino,²⁸ A.M.Cartacci,¹⁶ J.Casaus,²⁵ G.Castellini,¹⁶ F.Cavallari,³⁵ N.Cavallo,²⁸ C.Cecchi,¹⁹ M.Cerrada,²⁵ F.Cesaroni,²³ M.Chamizo,¹⁹ Y.H.Chang,⁴⁹ U.K.Chaturvedi,¹⁸ M.Chemarin,²⁴ A.Chen,⁴⁹ G.Chen,⁷ G.M.Chen,⁷ H.F.Chen,²⁰ H.S.Chen,⁷ X.Chereau,⁴ G.Chiefari,²⁸ L.Cifarelli,³⁷ F.Cindolo,⁹ C.Civinini,¹⁶ I.Clare,¹⁴ R.Clare,¹⁴ G.Coignet,⁴ A.P.Colijn,² N.Colino,²⁵ S.Costantini,⁸ F.Cotorobai,¹² B.Cozzoni,⁹ B.de la Cruz,²⁵ A.Csilling,¹³ S.Cucciarelli,³² T.S.Dai,¹⁴ J.A.van Dalen,³⁰ R.D'Alessandro,¹⁶ R.de Asmundis,²⁸ P.Déglon,¹⁹ A.Degré,⁴ K.Deiters,⁴⁵ D.della Volpe,²⁸ P.Denes,³⁴ F.DeNotaristefani,³⁵ A.De Salvo,⁴⁷ M.Diemoz,³⁵ D.van Dierendonck,² F.Di Lodovico,⁴⁷ C.Dionisi,³⁵ M.Dittmar,⁴⁷ A.Dominguez,³⁸ A.Doria,²⁸ M.T.Dova,^{18,†} D.Duchesneau,⁴ D.Dufournaud,⁴ P.Duinker,² I.Duran,³⁹ H.El Mamouni,²⁴ A.Engler,³³ F.J.Eppling,¹⁴ F.C.Erné,² P.Extermann,¹⁹ M.Fabre,⁴⁵ R.Faccini,³⁵ M.A.Falagan,²⁵ S.Falciano,^{35,17} A.Favara,¹⁷ J.Fay,²⁴ O.Fedin,³⁶ M.Felcini,⁴⁷ T.Ferguson,³³ F.Ferroni,³⁵ H.Fesefeldt,¹ E.Fiandrini,³² J.H.Field,¹⁹ F.Filthaut,¹⁷ P.H.Fisher,¹⁴ I.Fisk,³⁸ G.Forconi,¹⁴ L.Fredj,¹⁹ K.Freudenreich,⁴⁷ C.Furetta,²⁶ Yu.Galaktionov,^{27,14} S.N.Ganguli,¹⁰ P.Garcia-Abia,⁵ M.Gataullin,³¹ S.S.Gau,¹¹ S.Gentile,^{35,17} N.Gheordanescu,¹² S.Giagu,³⁵ Z.F.Gong,²⁰ G.Grenier,²⁴ O.Grimm,⁸ M.W.Gruenewald,⁸ M.Guida,³⁷ R.van Gulik,² V.K.Gupta,³⁴ A.Gurtu,¹⁰ L.J.Gutay,⁴⁴ D.Haas,⁵ A.Hasan,²⁹ D.Hatzifotiadou,⁷ T.Hebbeker,⁸ A.Hervé,¹⁷ P.Hidas,¹³ J.Hirschfelder,³³ H.Hofer,⁴⁷ G.Holzner,⁴⁷ H.Hoorani,³³ S.R.Hou,⁴⁹ I.Iashvili,⁴⁶ B.N.Jin,⁷ L.W.Jones,³ P.de Jong,² I.Josa-Mutuberría,²⁵ R.A.Khan,¹⁸ D.Kamrad,⁴⁶ M.Kaur,^{18,◇} M.N.Kienzle-Focacci,¹⁹ D.Kim,³⁵ D.H.Kim,⁴¹ J.K.Kim,⁴¹ S.C.Kim,⁴¹ J.Kirkby,¹⁷ D.Kiss,¹³ W.Kittel,³⁰ A.Klimentov,^{14,27} A.C.König,³⁰ A.Kopp,⁴⁶ I.Korolok,²⁷ V.Koutsenko,^{14,27} M.Kräber,⁴⁷ R.W.Kraemer,³³ W.Krenz,¹ A.Kunin,^{14,27} P.Ladron de Guevara,²⁵ I.Laktineh,²⁴ G.Landi,¹⁶ K.Lassila-Perini,⁴⁷ P.Laurikainen,²¹ A.Lavorato,³⁷ M.Lebeau,¹⁷ A.Lebedev,¹⁴ P.Lebun,²⁴ P.Lecomte,⁴⁷ P.Lecoq,¹⁷ P.Le Coultre,⁴⁷ H.J.Lee,⁸ J.M.Le Goff,¹⁷ R.Leiste,⁴⁶ E.Leonardi,³⁵ P.Levtchenko,³⁶ C.Li,²⁰ C.H.Lin,⁴⁹ W.T.Lin,⁴⁹ F.L.Linde,² L.Lista,²⁸ Z.A.Liu,⁷ W.Lohmann,⁴⁶ E.Longo,³⁵ Y.S.Lu,⁷ K.Lübelsmeyer,¹ C.Luci,^{17,35} D.Luckey,¹⁴ L.Lugnier,²⁴ L.Luminari,³⁵ W.Lustermann,⁴⁷ W.G.Ma,²⁰ M.Maity,¹⁰ L.Malgeri,¹⁷ A.Malinin,^{27,17} C.Maña,²⁵ D.Mangeol,³⁰ P.Marchesini,⁴⁷ G.Marian,¹⁵ J.P.Martin,²⁴ F.Marzano,³⁵ G.G.G.Massaró,² K.Mazumdar,¹⁰ R.R.McNeil,⁶ S.Mele,¹⁷ L.Merola,²⁸ M.Meschini,¹⁶ W.J.Metzger,³⁰ M.von der Mey,¹ A.Mihul,¹² H.Milcent,¹⁷ G.Mirabelli,³⁵ J.Mnich,¹⁷ G.B.Mohanty,¹⁰ P.Molnar,⁸ B.Monteoloni,^{16,†} T.Moulik,¹⁰ G.S.Muanza,²⁴ F.Muheim,¹⁹ A.J.M.Muijs,² M.Musy,³⁵ M.Napolitano,²⁸ F.Nessi-Tedaldi,⁴⁷ H.Newman,³¹ T.Niessen,¹ A.Nisati,³⁵ H.Nowak,⁴⁶ Y.D.Oh,⁴¹ G.Organtini,³⁵ R.Ostonen,²¹ C.Palomares,²⁵ D.Pandoulas,¹ S.Paoletti,^{35,17} P.Paolucci,²⁸ R.Paramatti,³⁵ H.K.Park,³³ I.H.Park,⁴¹ G.Pascale,³⁵ G.Passaleva,¹⁷ S.Patricelli,²⁸ T.Paul,¹¹ M.Pauluzzi,³² C.Paus,¹⁷ F.Pauss,⁴⁷ D.Peach,¹⁷ M.Pedace,³⁵ S.Pensotti,²⁶ D.Perret-Gallix,⁴ B.Petersen,³⁰ D.Piccolo,²⁸ F.Pierella,⁹ M.Pieri,¹⁶ P.A.Piroué,³⁴ E.Pistoletti,²⁶ V.Plyaskin,²⁷ M.Pohl,⁴⁷ V.Pojidaev,^{27,16} H.Postema,¹⁴ J.Pothier,¹⁷ N.Produit,¹⁹ D.O.Prokofiev,⁴⁴ D.Prokofiev,³⁶ J.Quartieri,³⁷ G.Rahal-Callot,^{47,17} M.A.Rahaman,¹⁰ P.Raics,¹⁵ N.Raja,¹⁰ R.Ramelli,⁴⁷ P.G.Rancoita,²⁶ G.Raven,³⁸ P.Razis,²⁹ D.Ren,⁴⁷ M.Rescigno,³⁵ S.Reucroft,¹¹ T.van Rhee,⁴³ S.Riemann,⁴⁶ K.Riles,³ A.Bohm,⁴⁷ J.Rodin,⁴² B.P.Roe,³ L.Romero,²⁵ A.Rosca,⁸ S.Rosier-Lees,⁴ J.A.Rubio,¹⁷ D.Ruschmeier,⁸ H.Rykaczewski,⁴⁷ S.Saremi,⁶ S.Sarkar,³⁵ J.Salicio,¹⁷ E.Sanchez,¹⁷ M.P.Sanders,³⁰ M.E.Sarakinos,²¹ C.Schäfer,¹ V.Schegelsky,³⁶ S.Schmidt-Kaerst,¹ D.Schmitz,¹ H.Schopper,⁴⁸ D.J.Schotanus,³⁰ G.Schwering,¹ C.Sciacca,²⁸ D.Sciarrino,¹⁹ A.Seganti,⁹ L.Servoli,³² S.Shevchenko,³¹ N.Shivarov,⁴⁰ V.Shoutko,²⁷ E.Shumilov,²⁷ A.Shvorob,³¹ T.Siedenburg,¹ D.Son,⁴¹ B.Smith,³³ P.Spillantini,¹⁶ M.Steuer,¹⁴ D.P.Stickland,³⁴ A.Stone,⁶ H.Stone,^{34,†} B.Stoyanov,⁴⁰ A.Straessner,¹ K.Sudhakar,¹⁰ G.Sultanov,¹⁸ L.Z.Sun,²⁰ H.Suter,⁴⁷ J.D.Swain,¹⁸ Z.Szillasi,^{42,¶} T.Sztricskai,^{42,¶} X.W.Tang,⁷ L.Tauscher,⁵ L.Taylor,¹¹ C.Timmermans,³⁰ Samuel C.C.Ting,¹⁴ S.M.Ting,¹⁴ S.C.Tonwar,¹⁰ J.Tóth,¹³ C.Tully,³⁴ K.L.Tung,⁷ Y.Uchida,¹⁴ J.Ulbricht,⁴⁷ E.Valente,³⁵ G.Vesztegombi,¹³ I.Vetlitsky,²⁷ D.Vicinanza,³⁷ G.Viertel,⁴⁷ S.Villa,¹¹ M.Vivargent,⁴ S.Vlachos,⁵ I.Vodopianov,³⁶ H.Vogel,³³ H.Vogt,⁴⁶ I.Vorobiev,²⁷ A.A.Vorobyov,³⁶ A.Vorvolakos,²⁹ M.Wadhwa,⁵ W.Wallraf,¹ M.Wang,¹⁴ X.L.Wang,²⁰ Z.M.Wang,²⁰ A.Weber,¹ M.Weber,¹ P.Wienemann,¹ H.Wilkens,³⁰ S.X.Wu,¹⁴ S.Wynhoff,¹ L.Xia,³¹ Z.Z.Xu,²⁰ B.Z.Yang,²⁰ C.G.Yang,⁷ H.J.Yang,⁷ M.Yang,⁷ J.B.Ye,²⁰ S.C.Yeh,⁵⁰ An.Zalite,³⁶ Yu.Zalite,³⁶ Z.P.Zhang,²⁰ G.Y.Zhu,⁷ R.Y.Zhu,³¹ A.Zichichi,^{9,17,18} F.Ziegler,⁴⁶ G.Zilizi,^{42,¶} M.Zöller,¹

- 1 I. Physikalisches Institut, RWTH, D-52056 Aachen, FRG[§]
III. Physikalisches Institut, RWTH, D-52056 Aachen, FRG[§]
 - 2 National Institute for High Energy Physics, NIKHEF, and University of Amsterdam, NL-1009 DB Amsterdam, The Netherlands
 - 3 University of Michigan, Ann Arbor, MI 48109, USA
 - 4 Laboratoire d'Annecy-le-Vieux de Physique des Particules, LAPP, IN2P3-CNRS, BP 110, F-74941 Annecy-le-Vieux CEDEX, France
 - 5 Institute of Physics, University of Basel, CH-4056 Basel, Switzerland
 - 6 Louisiana State University, Baton Rouge, LA 70803, USA
 - 7 Institute of High Energy Physics, IHEP, 100039 Beijing, China[△]
 - 8 Humboldt University, D-10099 Berlin, FRG[§]
 - 9 University of Bologna and INFN-Sezione di Bologna, I-40126 Bologna, Italy
 - 10 Tata Institute of Fundamental Research, Bombay 400 005, India
 - 11 Northeastern University, Boston, MA 02115, USA
 - 12 Institute of Atomic Physics and University of Bucharest, R-76900 Bucharest, Romania
 - 13 Central Research Institute for Physics of the Hungarian Academy of Sciences, H-1525 Budapest 114, Hungary[‡]
 - 14 Massachusetts Institute of Technology, Cambridge, MA 02139, USA
 - 15 Lajos Kossuth University-ATOMKI, H-4010 Debrecen, Hungary[¶]
 - 16 INFN Sezione di Firenze and University of Florence, I-50125 Florence, Italy
 - 17 European Laboratory for Particle Physics, CERN, CH-1211 Geneva 23, Switzerland
 - 18 World Laboratory, FBLJA Project, CH-1211 Geneva 23, Switzerland
 - 19 University of Geneva, CH-1211 Geneva 4, Switzerland
 - 20 Chinese University of Science and Technology, USTC, Hefei, Anhui 230 029, China[△]
 - 21 SEFT, Research Institute for High Energy Physics, P.O. Box 9, SF-00014 Helsinki, Finland
 - 22 University of Lausanne, CH-1015 Lausanne, Switzerland
 - 23 INFN-Sezione di Lecce and Università Degli Studi di Lecce, I-73100 Lecce, Italy
 - 24 Institut de Physique Nucléaire de Lyon, IN2P3-CNRS, Université Claude Bernard, F-69622 Villeurbanne, France
 - 25 Centro de Investigaciones Energéticas, Medioambientales y Tecnológicas, CIEMAT, E-28040 Madrid, Spain^b
 - 26 INFN-Sezione di Milano, I-20133 Milan, Italy
 - 27 Institute of Theoretical and Experimental Physics, ITEP, Moscow, Russia
 - 28 INFN-Sezione di Napoli and University of Naples, I-80125 Naples, Italy
 - 29 Department of Natural Sciences, University of Cyprus, Nicosia, Cyprus
 - 30 University of Nijmegen and NIKHEF, NL-6525 ED Nijmegen, The Netherlands
 - 31 California Institute of Technology, Pasadena, CA 91125, USA
 - 32 INFN-Sezione di Perugia and Università Degli Studi di Perugia, I-06100 Perugia, Italy
 - 33 Carnegie Mellon University, Pittsburgh, PA 15213, USA
 - 34 Princeton University, Princeton, NJ 08544, USA
 - 35 INFN-Sezione di Roma and University of Rome, "La Sapienza", I-00185 Rome, Italy
 - 36 Nuclear Physics Institute, St. Petersburg, Russia
 - 37 University and INFN, Salerno, I-84100 Salerno, Italy
 - 38 University of California, San Diego, CA 92093, USA
 - 39 Dept. de Física de Partículas Elementales, Univ. de Santiago, E-15706 Santiago de Compostela, Spain
 - 40 Bulgarian Academy of Sciences, Central Lab. of Mechatronics and Instrumentation, BU-1113 Sofia, Bulgaria
 - 41 Center for High Energy Physics, Adv. Inst. of Sciences and Technology, 305-701 Taejeon, Republic of Korea
 - 42 University of Alabama, Tuscaloosa, AL 35486, USA
 - 43 Utrecht University and NIKHEF, NL-3584 CB Utrecht, The Netherlands
 - 44 Purdue University, West Lafayette, IN 47907, USA
 - 45 Paul Scherrer Institut, PSI, CH-5232 Villigen, Switzerland
 - 46 DESY, D-15738 Zeuthen, FRG
 - 47 Eidgenössische Technische Hochschule, ETH Zürich, CH-8093 Zürich, Switzerland
 - 48 University of Hamburg, D-22761 Hamburg, FRG
 - 49 National Central University, Chung-Li, Taiwan, China
 - 50 Department of Physics, National Tsing Hua University, Taiwan, China
- § Supported by the German Bundesministerium für Bildung, Wissenschaft, Forschung und Technologie
‡ Supported by the Hungarian OTKA fund under contract numbers T019181, F023259 and T024011.
¶ Also supported by the Hungarian OTKA fund under contract numbers T22238 and T026178.
^b Supported also by the Comisión Interministerial de Ciencia y Tecnología.
[‡] Also supported by CONICET and Universidad Nacional de La Plata, CC 67, 1900 La Plata, Argentina.
◇ Also supported by Panjab University, Chandigarh-160014, India.
△ Supported by the National Natural Science Foundation of China.
† Deceased.

	$E_\gamma > 5 \text{ GeV}$			$E_\gamma > 1.3 \text{ GeV}$	$E_{\gamma_1} > 5 \text{ GeV}$
	Total	Barrel	Endcaps	$E_\gamma < 5 \text{ GeV}$	$E_{\gamma_2} > 1 \text{ GeV}$
Data	572	297	275	395	21
$\nu\bar{\nu}\gamma(\gamma)$	567.3	288.9	278.4	48.7	35.5
e^+e^- background	6.5	2.2	4.3	358.5	0.7
Cosmic background	3.1	1.1	2.0	3.6	0
Total expectation	576.9	292.2	284.7	410.8	36.2

Table 1: Number of events selected in data, Monte Carlo predictions for processes from e^+e^- collisions and contamination of cosmic ray background in the indicated kinematic regions.

\sqrt{s} (GeV)	N_ν
130.1	$2.63 \pm 0.40 \pm 0.10$
136.1	$2.98 \pm 0.49 \pm 0.14$
161.3	$3.68 \pm 0.53 \pm 0.09$
172.1	$4.24 \pm 0.65 \pm 0.09$
182.7	$3.13 \pm 0.26 \pm 0.05$
188.6	$2.94 \pm 0.15 \pm 0.04$
130 – 189	$3.05 \pm 0.11 \pm 0.04$
88 – 94	$2.98 \pm 0.07 \pm 0.07$
Average	3.011 ± 0.077

Table 2: Number of neutrino families measured from single photon events.

$\tilde{\chi}_1^0$ content	$m_{\tilde{e}_{L,R}}$ (GeV)	$m_{\tilde{\chi}_1^0}^{\text{lim}}$ (GeV)
Bino	150	87.9
Bino	100	90.8
Photino	150	88.3
Photino	100	91.1
Higgsino	—	89.0

Table 3: Neutralino mass limits for several neutralino compositions and selectron masses.

δ	2	3	4	5	6	7	8	9	10
ϵ (%)	42.8	40.7	38.9	37.6	36.5	35.5	34.7	34.0	33.4
$\sigma_{\gamma G}^{\text{lim}}$ (pb)	0.638	0.646	0.651	0.658	0.664	0.670	0.674	0.678	0.680
M_D (GeV)	1018	812	674	577	506	453	411	377	349

Table 4: Selection efficiency ϵ for $e^+e^- \rightarrow \gamma G$, upper cross section limit and lower limit on the energy scale M_D as a function of the number of extra dimensions δ .

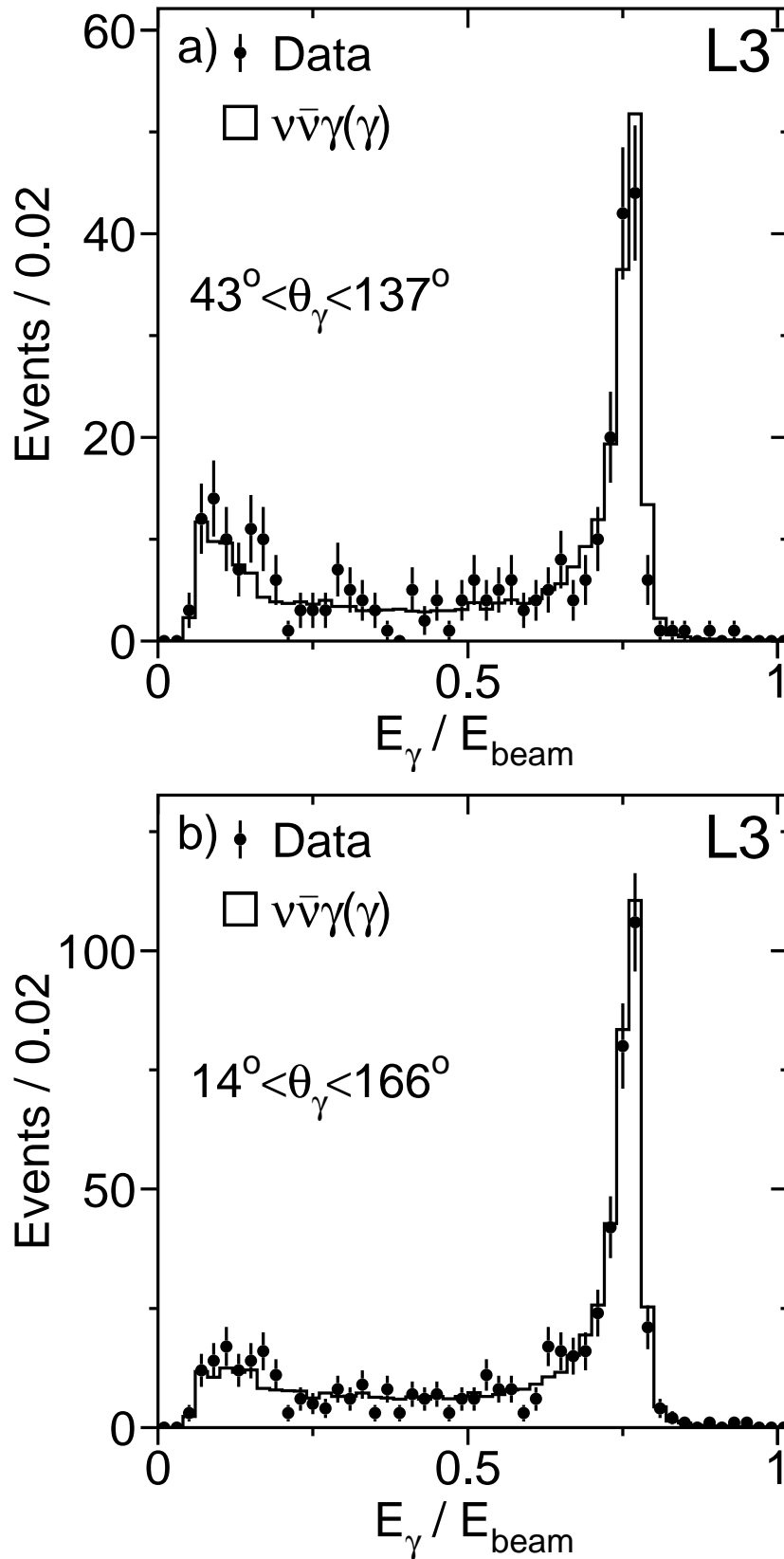


Figure 1: (a) Energy of the highest energetic photon normalised to the beam energy for single and multi-photon events at 189 GeV in the barrel region. (b) Same distribution with the endcaps included.

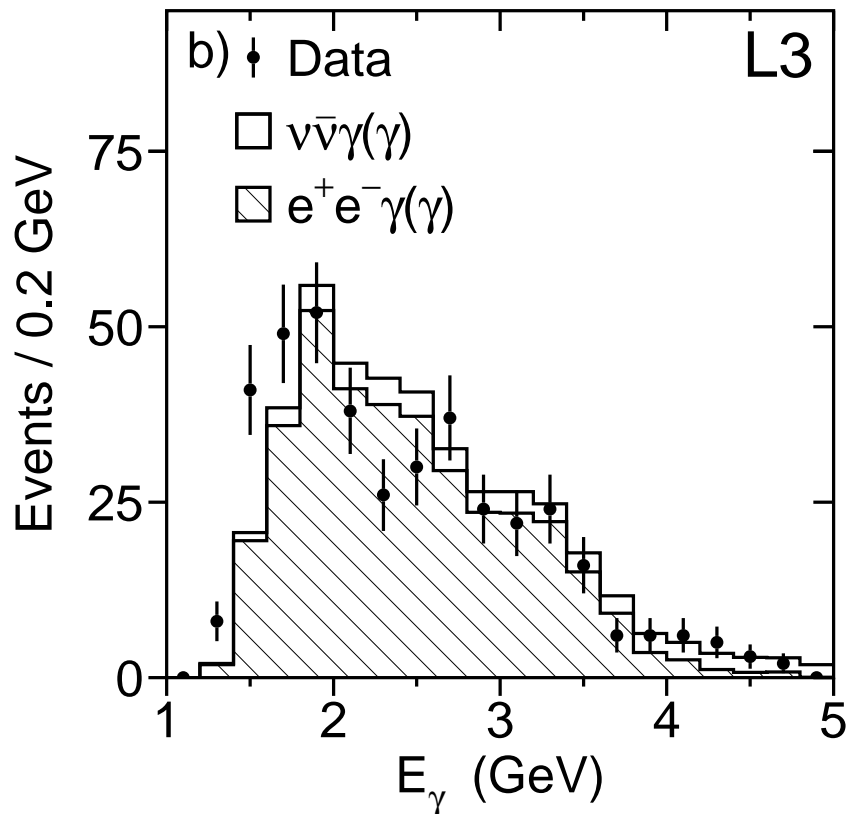
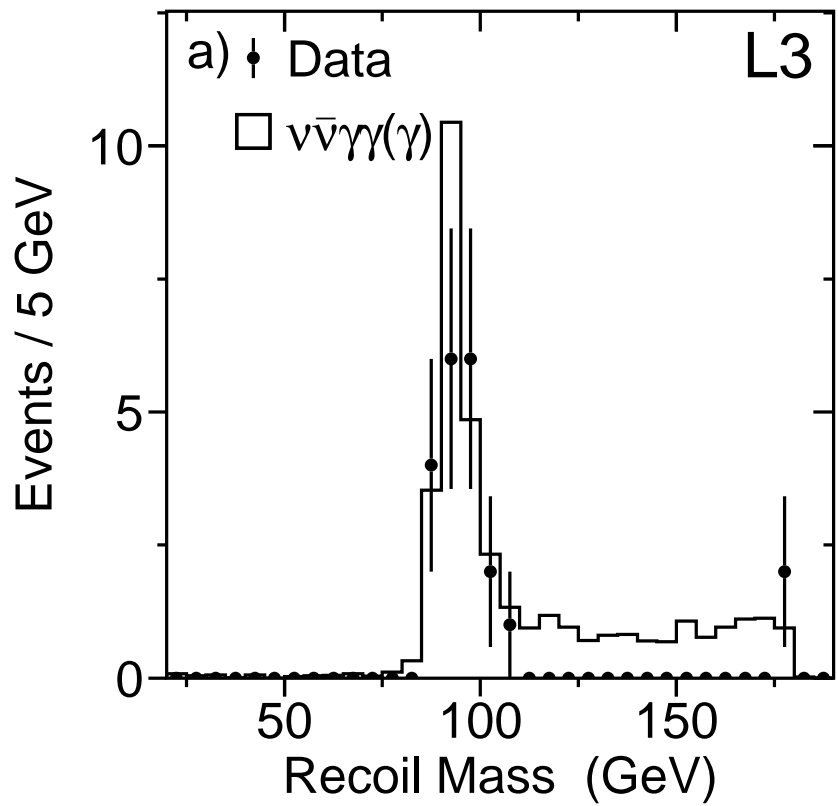


Figure 2: (a) Recoil mass for the multi-photon sample. (b) Low energy part of the energy spectrum of single photon events.

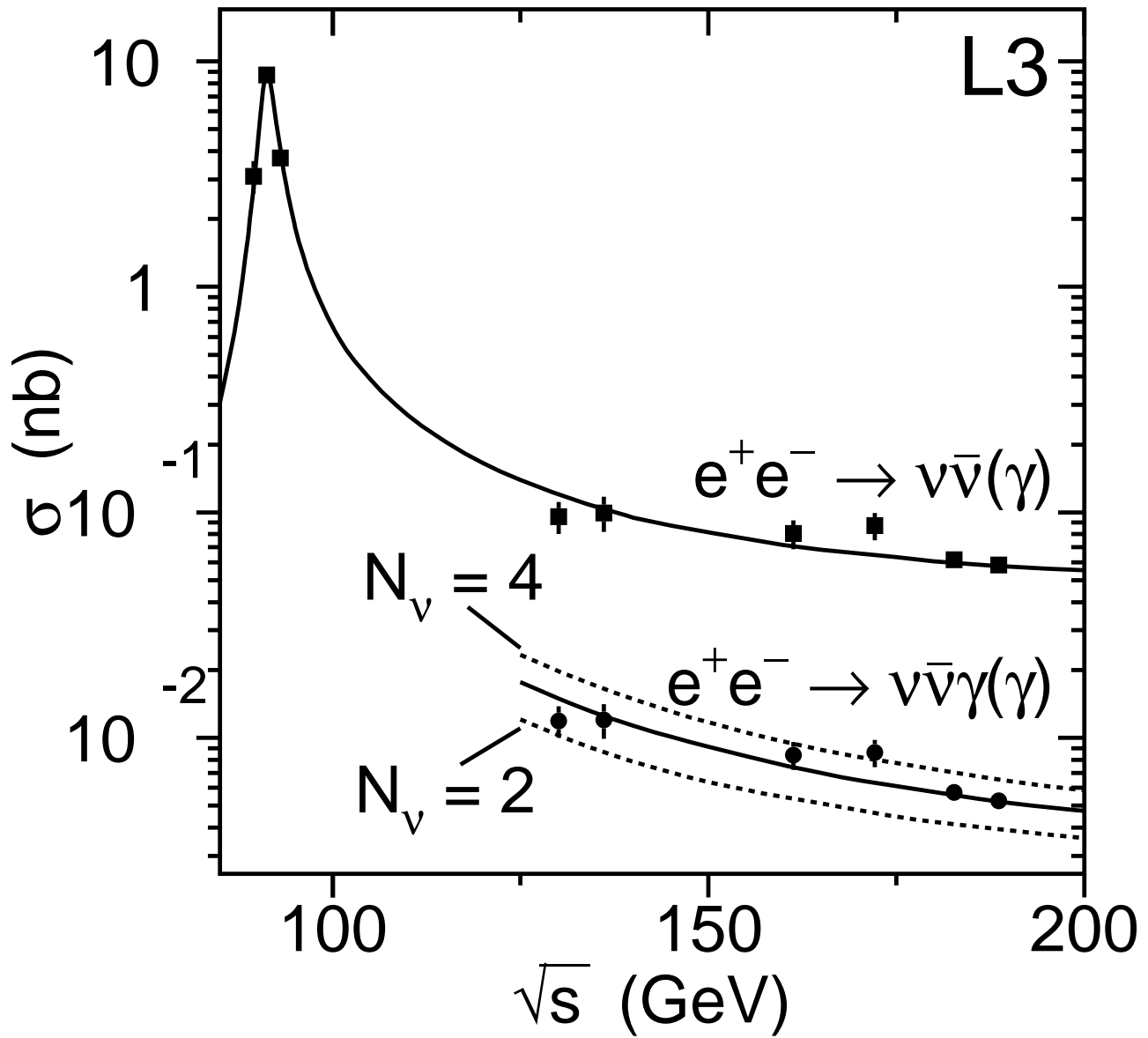


Figure 3: Production cross section of $e^+e^- \rightarrow \nu\bar{\nu}(\gamma)$ and $e^+e^- \rightarrow \nu\bar{\nu}\gamma(\gamma)$ as a function of the centre-of-mass energy. Points with error bars represent the $\nu\bar{\nu}\gamma(\gamma)$ measurements and squares with error bars are the extrapolation to $\nu\bar{\nu}(\gamma)$. The full line is the theoretical prediction for $N_\nu = 3$ and dashed lines are predictions for $N_\nu = 2, 4$ as indicated.

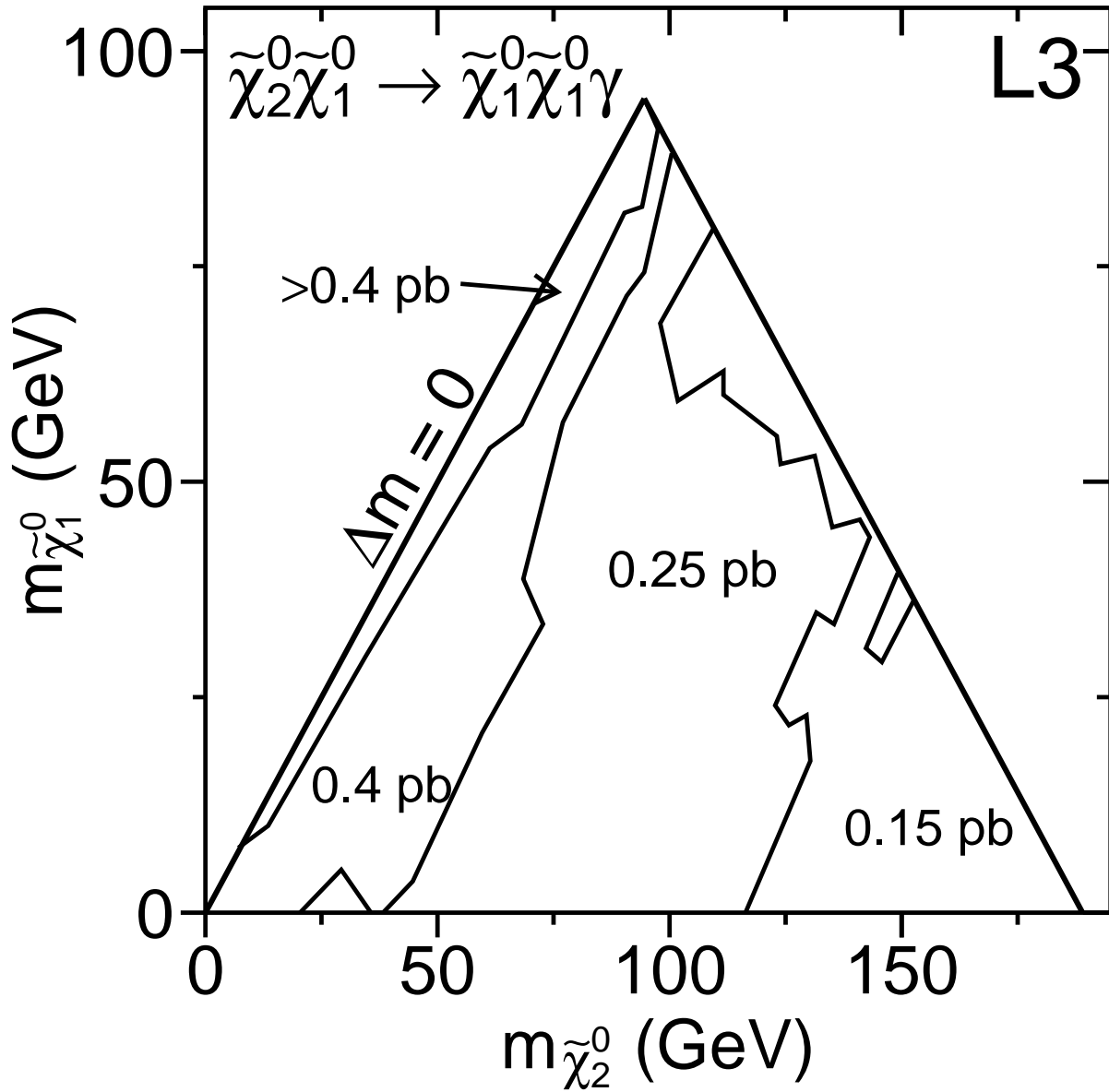


Figure 4: Upper limits on the production cross section in picobarn for the process $e^+e^- \rightarrow \tilde{\chi}_2^0 \tilde{\chi}_1^0 \rightarrow \tilde{\chi}_1^0 \tilde{\chi}_1^0 \gamma$ assuming 100% branching ratio for $\tilde{\chi}_2^0 \rightarrow \tilde{\chi}_1^0 \gamma$.

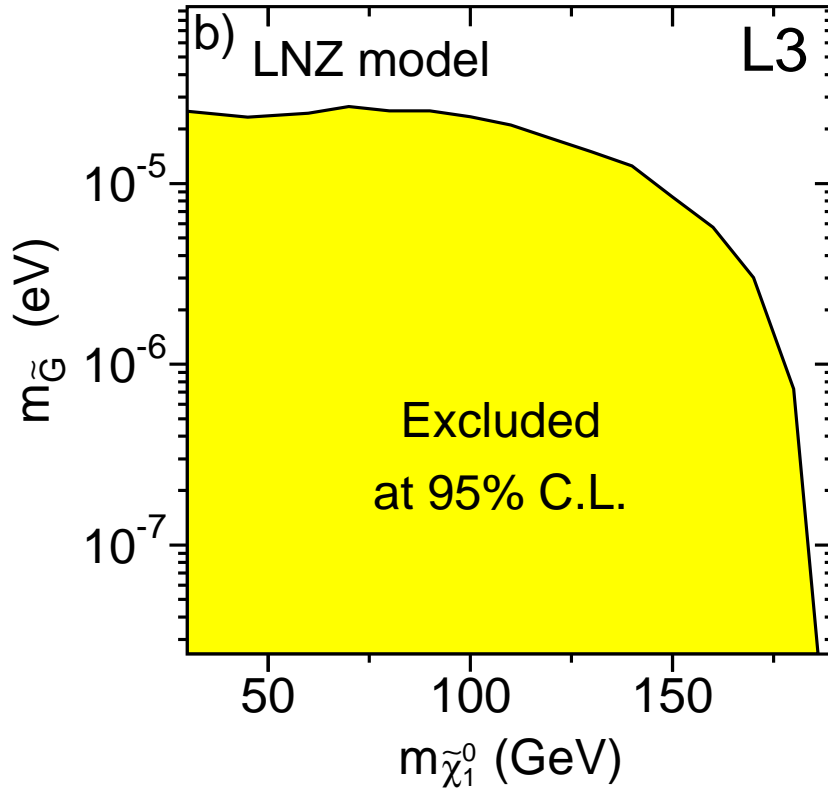
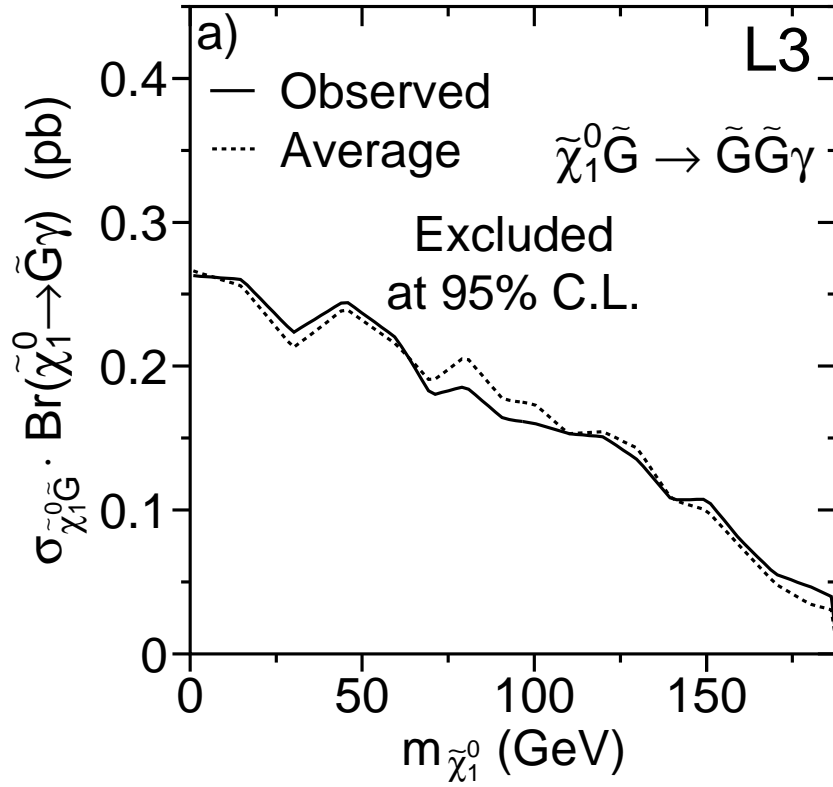


Figure 5: (a) Upper limits on the production cross section for the process $e^+e^- \rightarrow \tilde{G}\tilde{\chi}_1^0 \rightarrow \tilde{G}\tilde{G}\gamma$ and average limit obtained using Monte Carlo trials with background only. (b) Region excluded in the LNZ model in the plane $m_{\tilde{G}}$ versus $m_{\tilde{\chi}_1^0}$.

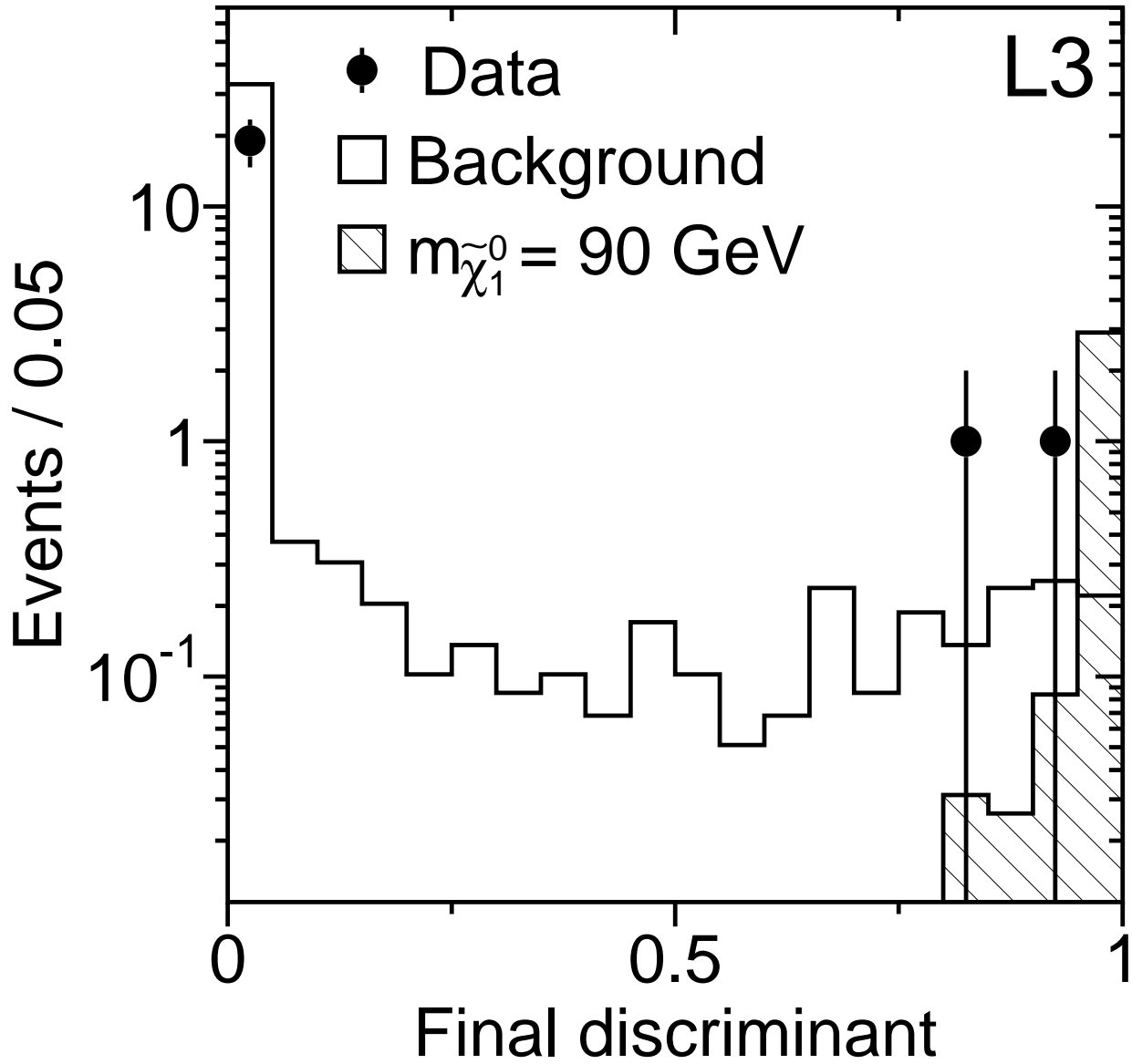


Figure 6: Discriminant variable for $\tilde{\chi}_1^0 \tilde{\chi}_1^0 \rightarrow \tilde{G} \tilde{G} \gamma \gamma$ with $m_{\tilde{\chi}_1^0} = 90$ GeV. The signal corresponds to the upper limit of 3.15 events derived for this mass point.

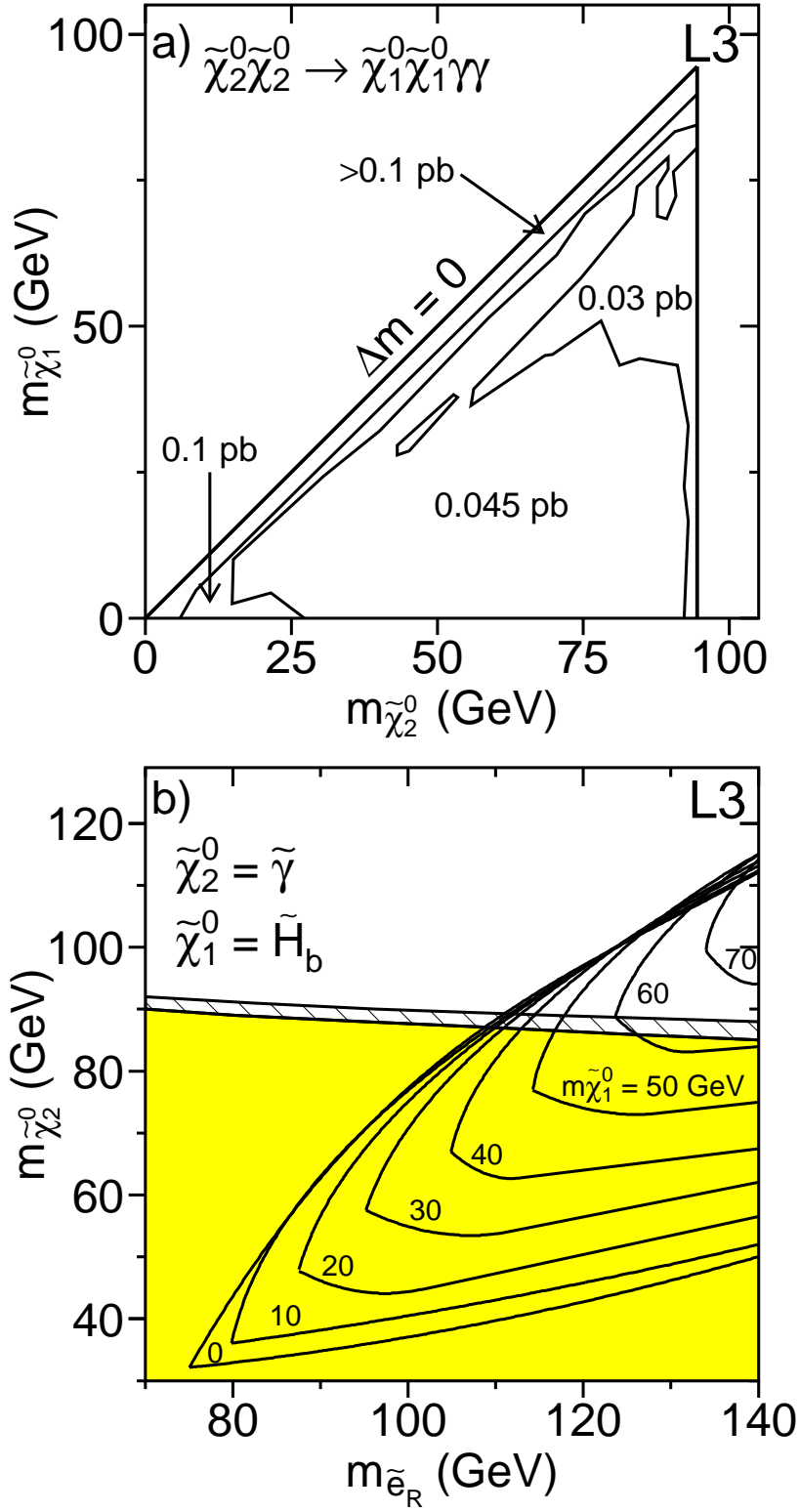


Figure 7: (a) Upper limits on the production cross section in picobarn for the process $e^+e^- \rightarrow \tilde{\chi}_2^0 \tilde{\chi}_2^0 \rightarrow \tilde{\chi}_1^0 \tilde{\chi}_1^0 \gamma \gamma$. (b) Excluded region in the neutralino selectron mass plane. The shaded region corresponds to $m_{\tilde{e}_L} \gg m_{\tilde{e}_R}$ and the hatched region is additionally excluded when $m_{\tilde{e}_L} = m_{\tilde{e}_R}$. Regions kinematically allowed for the CDF event [30] as a function of $m_{\tilde{\chi}_1^0}$ are indicated, where $\tilde{\chi}_1^0 = \tilde{H}_b = \tilde{H}_1^0 \sin \beta + \tilde{H}_2^0 \cos \beta$.

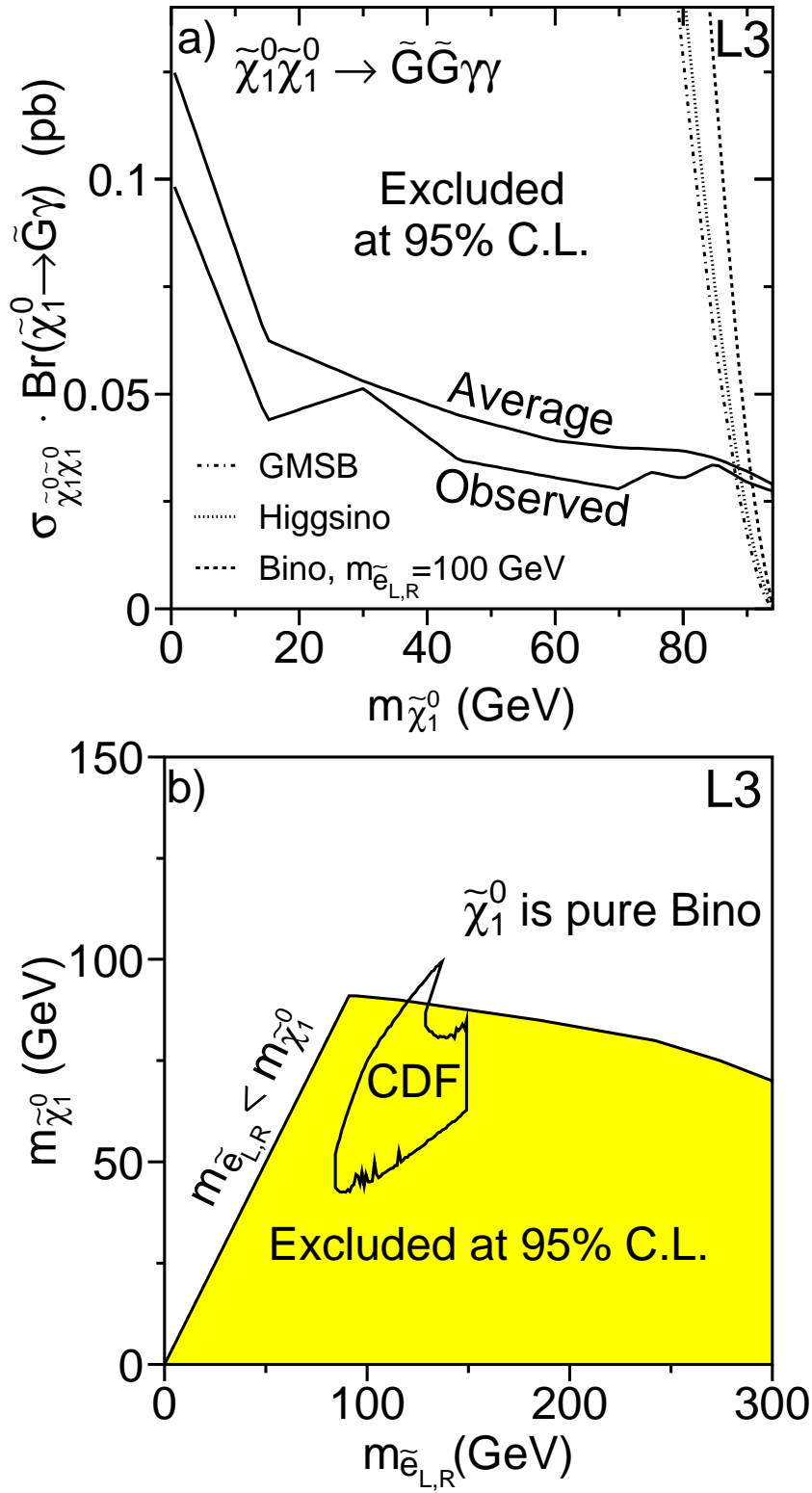


Figure 8: (a) Upper limit on the cross section for $e^+e^- \rightarrow \tilde{\chi}_1^0 \tilde{\chi}_1^0 \rightarrow \tilde{G}\tilde{G}\gamma\gamma$. Theoretical predictions for two extreme cases of $\tilde{\chi}_1^0$ composition and for the most conservative GMSB prediction are also shown. (b) Excluded region for a pure bino neutralino model compared to the region consistent with the supersymmetric interpretation of the CDF event in the scalar electron scenario [31].